ACS OMEGA

http://pubs.acs.org/journal/acsodf

Article

Novel Thermoelectric Character of Rhenium Carbonitride, ReCN

Abdul M. Reyes,* Jesús L. A. Ponce-Ruiz, Eduardo S. Hernández, and Armando Reyes Serrato*

Cite This: *ACS Omega* 2021, 6, 18364−18369

Read Online

ACCESS | Metrics & More | Article Recommendations

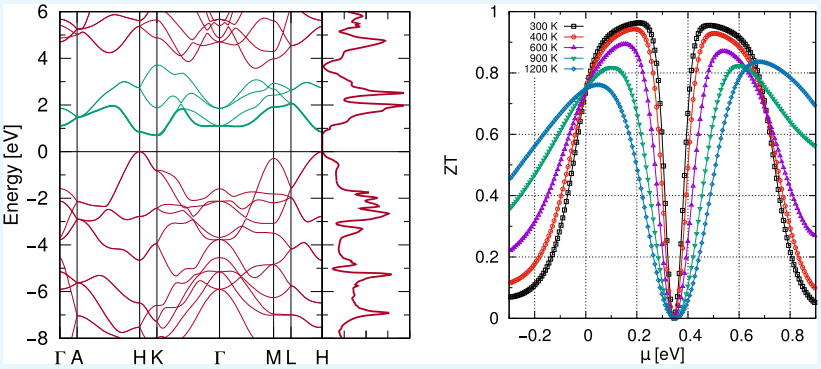

ABSTRACT: Nowadays, it is very important to study and propose new mechanisms for generating electricity that are environmentally friendly, in addition to using renewable resources. Thermoelectric (TE) devices are fabricated with materials that can convert a temperature difference into electricity, without the need for rotating parts. In this work, we report the TE properties of rhenium carbonitride (ReCN) as an important feature of a hard and thermodynamically stable material of band gap Δ_g = 0.626 eV. We use the electronic band structure behavior near the Fermi energy with the Seebeck coefficient to estimate the figure of merit ZT based on Boltzmann transport theory to characterize this property. Our results show that this compound has interesting TE properties among 300 and 1200 K for p- and n-type doping.

INTRODUCTION

Development and understanding of thermoelectric (TE) materials has become an important topic for materials chemistry, physics, and engineering,[1] due to the large number of applications and/or devices, that might be used in energy and cooler generators, either to convert heat into electricity or as heat pumps. In this sense, the TE conversion has received a renewed interest due to the development of materials that show high TE conversion factors and improving recovery energy power from heat.[2] Therefore, it is important to work not only in the deep understanding of how materials are combined but also in its equilibrium transport to finally understand how the heat, charge transport, and scattering occur, to propose clean devices, which mitigate environmental changes.

The dimensionless figure of merit can be expressed in the form $ZT = \sigma S^2 T/\kappa$, where S is the Seebeck coefficient, σ is the electrical conductivity, T is the absolute temperature, and κ is the sum of κ_e and κ_l which are electronic and lattice thermal conductivity, respectively. As the ZT quantifies the performance of a TE, it is necessary to maximize the power factor $S^2\sigma$ and minimize thermal conductivity ($\kappa = \kappa_e + \kappa_l$), but all these terms depend strongly on electronic structure, charge carrier concentration, and crystalline structure, so that finding new compounds with large values of ZT is a complex task.[3,4] There are two main approaches to consider: first, to search for intrinsic materials and second, to improve the TE properties of known materials by physically modifying them.[5] Using the first approach, Kagdada et al.[6] studied the electronic and TE properties for the stable phases of GeTe, obtaining ZT = 0.7 at 1300 K, making it a promising candidate. On the other hand, Hong et al.[7] maximized the TE behavior of GeTe by doping with Sb and Sn obtaining a ZT = 2.2 at 780 K. These works, among others, show that the properties of TE determine their application. In this regard, an important application is for TE generators (TEGs), which exploit the Seebeck effect to convert heat directly into electrical energy. A TEG is composed of a stack of p- and n-type TE semiconductors.[8] These TEGs are used in aerospace missions and, in conjunction with radioisotopes or heat generated by motors, become an electrical source capable of operating for long periods of time. Also,

Received: May 5, 2021
Accepted: June 28, 2021
Published: July 9, 2021

using microelectronics, flexible TEGs have been incorporated to supply power to electrocardiographic systems, but their large-scale application remains limited due to their low efficiency.[9] In addition, many TEs, which are developing in the process of achieving high ZT values for TE materials, deteriorate at temperatures near peak ZT, which is a serious challenge in making reliable TE devices,[1] also when TE materials could be exposed to thermal and mechanical stresses which may cause reduction in device efficiency.[4,10−13]

Currently, it has been working on the search for new materials that can be used as TE, able to compete against current power generators. Since the semiconductor and mechanical properties have been theoretically reported,[14] where it is predicted that Vickers hardness of the ReCN for two phases is found to be more than 40 GPa, it is suggested that it could be a candidate for superhard materials. Also, ReCN has been reported as a new 2D material with strong structural rearrangement due to reducing dimension effects and conductor character due to d orbitals of Re atoms.[15] In the present work, we have investigated the transport properties of hexagonal ReCN in a bulk configuration and considering it as a p- and n-type semiconductor, finding the highest intrinsic TE behavior, with a symmetric character for p- and n-type doped systems and ZT = 0.978 at 300 K among others.

RESULTS AND DISCUSSION

Structural Properties. The optimized stable structure of the ReCN is shown in Figure 1. This hexagonal three-dimensional configuration has calculated lattice parameters of $a = b = 2.892$ Å and $c = 7.843$ Å, respectively. In Figure 1a, the three-dimensional ReCN is represented,[16] where it is easy to see how the Re atoms are placed inside boxes formed by C and N atoms located alternately in the z direction, separated by a double layer also of C and N atoms, with a distance of 1.407 Å approximately. Figure 1b,c shows top and side views particularly noting the honeycomb configurations with Re atoms placed in the center surrounded by C and N atoms. Likewise, the existence of sublayers divided by C and N atoms, in accordance with previous works,[14,15] was also reported, among other things, such as its semiconductor character, excellent mechanical properties with the large volume modulus, shear modulus, and ideal strength.

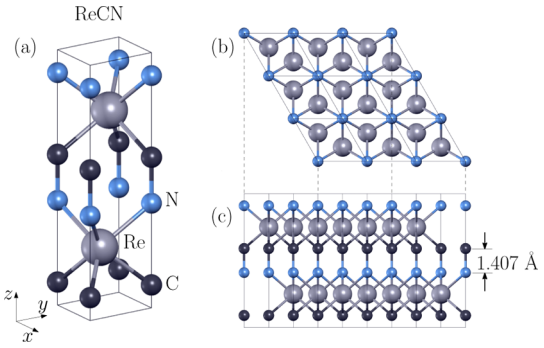

Figure 1. Bulk-optimized hexagonal structure of ReCN in a configuration of two unitary formulas and space group $P6_3cm$ (186), (a) three-dimensional view, (b) top view, and (c) side view.

Figure 2a shows the phonon dispersion of ReCN along the path shown in Figure 2b, from the spectrum obtained, it can be noted that all bands start above 0 THz, showing dynamical stability of the compound, with no negative frequency modes and acoustic bands separated from the optical ones. Thus, from our results, it is demonstrated that the hexagonal ReCN in the bulk configuration is a TE material with excellent mechanical properties. We hope that this will motivate, for example, experimental researchers using the high-pressure and high-temperature techniques in diamond anvil cells[17] to attempt the synthesis of ReCN since this technique has proven to be useful to obtain new materials.[18]

Electronic Properties. Figure 3 shows the calculated band structure of ReCN (in the same path shown in Figure 2b), where we want to point out the flat region between K−Γ−M, which has dispersion less than 0.1 eV. Degenerate states can be seen in the lower part of the conduction band, around the Γ point, especially at the level near 1 eV, where this heavy band could give hints of p- or n-type TE behavior. As we will show later, this symmetry breaking should generate a high Seebeck coefficient, which in this case is disadvantaged by the shift of the Fermi level toward the valence band.[19]

Since the TE effects can be predicted from the presence of flat bands,[20] they will gradually contribute to the charge carrier transport increasing the Seebeck coefficient as the temperature increases.[21] In Figure 4, we show the total density of states (DOS) and to understand which atomic species contributes the most to this band, we plot the projections of the DOS per atomic species, calculated for the system with the hexagonal ReCN structure. In this sense, the projected DOS shows that the peak of the band, which is present at 1 eV and is part of the intense bands that are between 1 and 4 eV, is mainly composed by the overlap of the degenerated Re $d_{x^2-y^2} + d_{xy}$ states, and the electrons occupying this band will have the same energy. On the other hand, the band gap of this system in the ground state was calculated to be $\Delta_g = 0.626$ eV, an important feature for a semiconductor.

Thus, the band plane at ∼1 eV between K−Γ−M and band gap less than 1 eV, obtained from the band structure, showed that ReCN has important characteristics to be considered TE.

TE Properties. In a TE, there are free electrons and holes, which carry charge or heat. The Seebeck effect is defined by the electric potential (voltage) produced by a temperature difference, and the link between the voltage developed and the temperature gradient ($\Delta V/\Delta T$) is related to the thermopower or Seebeck coefficient (S), which is positive or negative. The Seebeck coefficient is lower for metals (μV/K) and higher for semiconductors (10^2 μV/K).[22,23]

Based on the calculated band structure, the electric transport properties can be calculated using Boltzmann transport theory. If the relaxation time τ is taken to be a constant,[4] the S can be obtained independent of τ.

As mentioned in the models and computational methods, the virtue of using BoltzTrap is that S can be calculated without knowing the value of the relaxation time. In our case, this is of vital importance due to the thermoelectricity in ReCN is a new property and, since it remains to be synthesized, it is not known experimentally.

Figure 5a shows the S for various temperatures, where the dependence on doping can be seen. In the temperature range selected, the maximum value is obtained for 300 K at 0.291 eV with p-type doping; thus, at 0.379 eV, there is a transition to n-type reaching a negative maximum at 0.407 eV, consistent with other TE behaviors of GeSe, SnSe, PbSe,[24] and α-Ag_2S which is an inorganic semiconductor,[25] relativistic Na_2AgSb semimetal,[19] and hybrid perovskites $CH_3CH_2NH_3GeI_3$[26] among others.

https://doi.org/10.1021/acsomega.1c02357
ACS Omega 2021, 6, 18364−18369

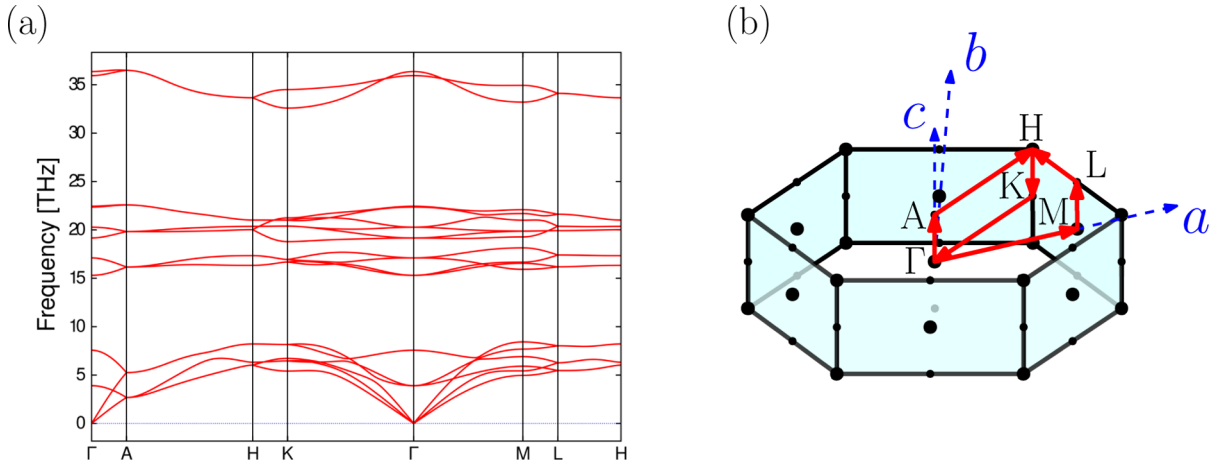

Figure 2. (a) Phonon dispersion of ReCN in the bulk configuration along the (b) *k*-points path in the first Brillouin zone. From the phonon spectrum, it can be seen that all bands start above 0 THz, showing dimensional stability of the network with no negative frequency modes and with the acoustic bands separated from the optical bands.

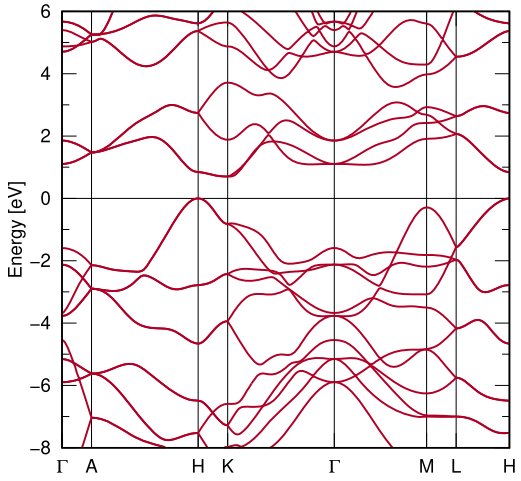

Figure 3. Calculated band structure of hexagonal ReCN shows a flat region between K−Γ−M, with no dispersion at 0.1 eV, extending around the Γ point, which is key to determine ReCN as a TE.

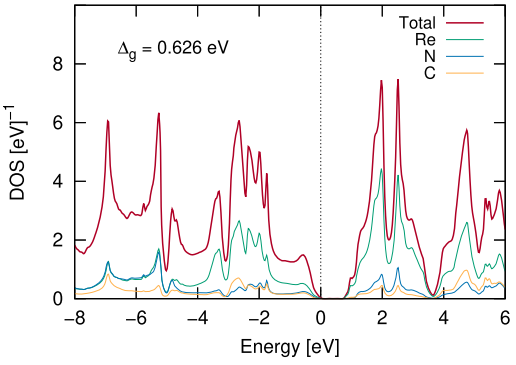

Figure 4. DOS of hexagonal ReCN. The Fermi level is indicated with broken line $E = 0$. The band extending from 0.5 to 4.0 eV above the Fermi level is composed mainly of Re $d_{x^2-y^2} + d_{xy}$ states.

The potential difference created by the Seebeck effect between two conductors or semiconductors, when there is a temperature gradient, is due to the movement of free electrons from the high-temperature region to the low-temperature region, causing a TE force which in our case is ∼mV per kelvin.

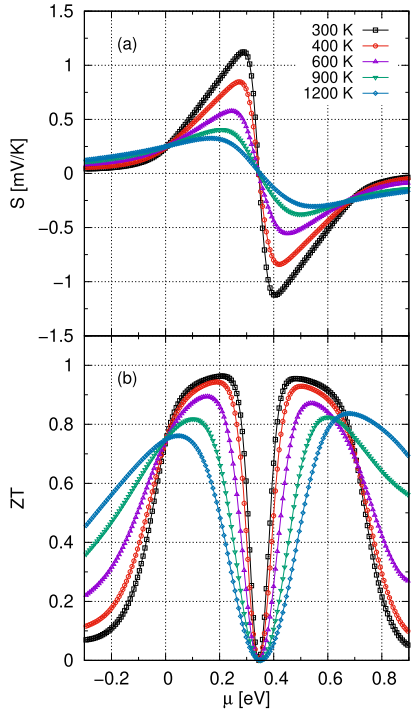

Figure 5. TE character of hexagonal ReCN. (a) Thermopower or Seebeck coefficient, where the highest value at room temperature is shown, p-type to n-type transition occurs between 0.325 and 0.379 eV. (b) Figure of merit, where the performance at various temperatures is compared, and it can be seen that the compound could work up to temperatures of the order of 1200 K.

Therefore, the TE efficiency depends on the composite having high *S* and this in turn depends on the shape of the DOS near the band edges, as the electronic behavior is affected by temperature variations. As can be seen in Figure 5a, *S* is positive for holes and negative for electrons, showing that ReCN can be good as p-type and n-type and operates with good TE properties—for 300 K—, between chemical potential $\mu = 0.291$ and 0.407 eV.

High-performance TEs, when ZT ∼ 1 or larger, are considered as good candidates for devices.[3] According to the definition of ZT given above, a key prerequisite is that a good

https://doi.org/10.1021/acsomega.1c02357
ACS Omega 2021, 6, 18364−18369

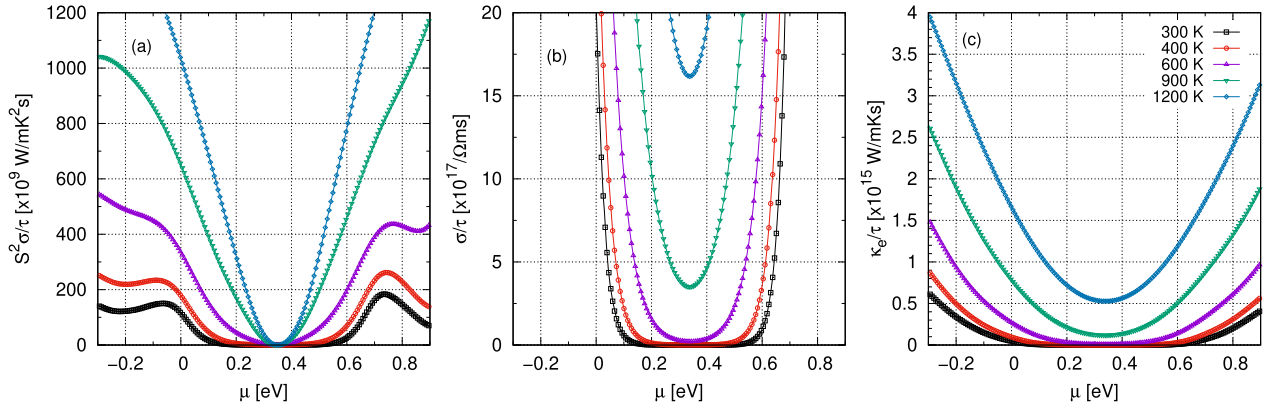

Figure 6. TE properties as a function of chemical potential (μ), to estimate the figure of merit ZT for ReCN at different temperatures. (a) Power factor (PF = $S^2\sigma/\tau$), (b) electrical conductivity (σ/τ), and (c) electronic thermal conductivity (κ_e/τ).

Table 1. Summary of TE Properties of ReCN for Different Temperatures[a]

T [K]	μ [eV]	N [e/u.c.]	ZT	PF × 10^9 [W/mK^2 s]	S [mV/K]	σ/τ [1/Ω ms]	κ_e/τ [W/mK s]
				p-Type			
300	0.237	3.200×10^{-7}	0.978	0.289	0.993	2.923×10^{14}	8.856×10^{10}
400	0.209	1.002×10^{-5}	0.960	5.089	0.731	9.523×10^{15}	2.121×10^{12}
600	0.166	3.014×10^{-4}	0.911	68.645	0.493	2.828×10^{17}	4.523×10^{13}
900	0.114	3.255×10^{-3}	0.828	358.819	0.349	2.936×10^{18}	3.901×10^{14}
1200	0.053	1.288×10^{-2}	0.764	855.735	0.280	1.091×10^{19}	1.344×10^{15}
				n-Type			
300	0.461	-6.200×10^{-7}	0.973	0.436	−0.982	4.522×10^{14}	1.344×10^{11}
400	0.489	-1.997×10^{-5}	0.950	7.318	−0.716	1.427×10^{16}	3.082×10^{12}
600	0.529	-0.566×10^{-3}	0.889	89.196	−0.472	4.003×10^{17}	6.023×10^{13}
900	0.597	-6.760×10^{-3}	0.825	453.501	−0.318	4.486e × 10^{18}	4.944×10^{14}
1200	0.685	-3.04×10^{-2}	0.836	1150.869	−0.253	1.800e × 10^{19}	1.652×10^{15}

[a]It is noted that as temperature increases, PF, σ/τ, and κ_e/τ also increase. While the absolute value of N and S increases and decreases, respectively.

TE has high S in an interesting temperature range (generally on the order of 200 μV/K or larger) with low thermal conductivity and good charge mobility.

We calculated ZT of the ReCN, as a function of the chemical potential μ for different temperatures (300, 400, 600, 900, and 1200 K), as shown in Figure 5b. In order to understand the TE properties, the calculations were performed keeping τ as an unknown property of this compound. For p-type ReCN, the maximum ZT at 300 K is 0.978, while for n-type ReCN, the maximum ZT is 0.973. Although these values do not correspond to the maximum power factors, defined as PF = $S^2\sigma/\kappa$ (see Figure 6a), it can be seen from Table 1 that the maximum S corresponds to the lowest value of $\kappa_e/\tau \sim 10^{10}$ and $\sigma/\tau \sim 10^{14}$, corresponding with a low amount of charge carriers ($\sim 10^{-7}$) among all the temperatures we expose.

To better understand the TE performance of ReCN, Figure 7 shows the ZT for the p- and n-type doping shown in Table 1, for the chemical potentials μ at which the values of 300 and 1200 K are reached. The light and dark blue lines for p-type doping and the red and orange lines for n-type doping show that at 1200 K, ReCN performs better as n-type, while near 300 K, as p- and n-type.

Table 1 summarizes the results at the temperatures selected in this analysis, from which it can be seen that p- or n-type doping has a better performance between 300 and 900 K, appearing symmetrical between μ = 0 and 0.7 eV. This symmetry can be seen in Figure 6b,c, since, for almost all temperatures, the difference in the order of magnitude between σ/τ and κ_e/τ is $\sim 10^4$. Thus, the ZT values obtained for ReCN indicate that it could be a good candidate, being a thermodynamically stable material with exceptional mechanical properties, to be considered as TE.

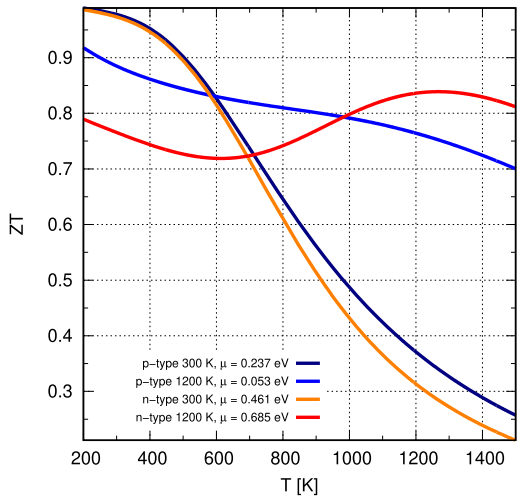

Figure 7. TE performance of ReCN, where the figure of merit ZT is shown as a function of T for four chemical potentials μ, corresponding to 300 and 1200 K, for both p- and n-type doping, as shown in Table 1. The light and dark blue lines represent p- and the red and orange lines represent n-type doping.

https://doi.org/10.1021/acsomega.1c02357
ACS Omega 2021, 6, 18364−18369

CONCLUSIONS

Currently, work has been carried out in the search for new materials that can be used as TEs, capable of competing with current power generators. In this work, we have studied the intrinsic transport properties of bulk ReCN, to see if it can be considered as TEs, showing comparable characteristics with the stable phases of GeTe which has a ZT = 0.7 at 1300 K, since our compound ReCN has ZT ∼ 0.8 at 1200 K.

Thus, we find a flat region between K−Γ−M, at about 1 eV, with a low dispersion (∼0.1 eV) indicating that the ReCN system could be a TE material. We conclude that this region is mostly composed of $d_{x^2-y^2} + d_{xy}$ degenerate states and also that the gap in the ground state is Δ_g = 0.626 eV.

To test the above mentioned prediction, a study of the TE properties was performed, resulting in ReCN having high Seebeck coefficients as a function of chemical potential in the range between μ = 0.2 and 0.5 eV, with σ/τ and κ_e/τ increasing with temperature, although κ_e/τ remains lower than σ/τ on the order of $\sim 10^4$. Consequently, ReCN has symmetry around the p- and n-type transition points with ZT ∼ 1, for intrinsic TE behavior at low temperature, which means that it can be considered as a TE, serving almost equally as a donor or acceptor.

Therefore, the ReCN compound could be considered as a TE material with excellent mechanical properties, which hopefully can be synthesized in the future.

MODELS AND COMPUTATIONAL METHODS

Our first-principles calculation were performed with the WIEN2k package,[27] which allow us to perform electronic structure calculations using density functional theory. It is based on the full-potential augmented plane-wave method. We determined the values needed to check that our structure has the correct symmetry, by first calculating the nearest-neighbor distance taking into account the atomic radius to avoid overlapping of atomic sites. The separation energy between the core and valence states was set to −6.5 Ry, and the generalized gradient approximation with Perdew−Burke−Ernzerhoff (PBE) exchange−correlation functions[28] was used. Our calculations were performed in the Brillouin zone with 25 × 25 × 7 uniform k-point mesh, due to a negligible difference in the total energy, our calculations were performed without taking into account spin−orbit coupling and a convergence criterion of 10^{-4} Ry was used. In addition, to show the stability of ReCN, the phonon dispersion was calculated using phonopy,[29] creating six supercells, with displacements of 4 × 4 × 2 unit cells of 64 unit formulas. These calculations were performed with the VASP code[30,31] finding the force constants from the forces on the atoms, with the finite-difference method, using a kinetic energy cutoff of 520 eV and a Monkhorst−Pack scheme[32] in the Brillouin zone with 2 × 2 × 2 uniform k-point mesh and 10^{-8} eV as the convergence energy threshold.

In the present work, TE properties such as Seebeck coefficients and electronic conductivity are calculated using the BoltzTrap[33] code. Next, we made a temperature sweep from 1 to 2000 K, with different doping values, in order to calculate the thermopower or Seebeck coefficient and estimate the ZT behavior.

AUTHOR INFORMATION

Corresponding Authors

Abdul M. Reyes − *Centro de Nanociencias y Nanotecnología, Universidad Nacional Autónoma de México, Ensenada, Baja California 22800, Mexico;* orcid.org/0000-0001-6997-0054; Phone: +52(646) 175-0650; Email: reyesabdul@iim.unam.mx

Armando Reyes Serrato − *Centro de Nanociencias y Nanotecnología, Universidad Nacional Autónoma de México, Ensenada, Baja California 22800, Mexico; Donostia International Physics Center, 20018 Donostia-San Sebastián, Spain*; Email: armando@cnyn.unam.mx

Authors

Jesús L. A. Ponce-Ruiz − *Centro de Investigación en Materiales Avanzados, S.C. (CIMAV), 31136 Chihuahua, Mexico*

Eduardo S. Hernández − *Posgrado en Nanociencias, CICESE-UNAM, Ensenada, Baja California 22860, Mexico*

Complete contact information is available at: https://pubs.acs.org/10.1021/acsomega.1c02357

Notes

The authors declare no competing financial interest.

ACKNOWLEDGMENTS

This work was partially supported by grants UNAM-PAPIIT-IN105019 and IG200320. A.M.R. is grateful to UNAM-PAPIIT-IG200320 for the fellowship. J.L.A.P.-R. is grateful to CONACyT for the fellowship CVU-562553. E.S.H is grateful to CONACYT for scholarship and Posgrado de Nanociencias for financial support and the projects DGAPA-UNAM, PAPIIT-IN112917, and LANCADUNAM-DGTIC-084. A.R.S. is grateful to PASPA-DGAPA-UNAM for the sabbatical scholarship and to the DIPC for their support during the research stay.

REFERENCES

(1) Recatala-Gomez, J.; Suwardi, A.; Nandhakumar, I.; Abutaha, A.; Hippalgaonkar, K. Toward Accelerated Thermoelectric Materials and Process Discovery. *ACS Appl. Energy Mater.* **2020**, *3*, 2240−2257.

(2) LeBlanc, S.; Yee, S. K.; Scullin, M. L.; Dames, C.; Goodson, K. E. Material and Manufacturing Cost Considerations for Thermoelectrics. *Renewable Sustainable Energy Rev.* **2014**, *32*, 313−327.

(3) Bilal, M.; Khan, B.; Rahnamaye Aliabad, H. A.; Maqbool, M.; Jalai Asadabadi, S.; Ahmad, I. Thermoelectric Properties of $SbNCa_3$ and $BiNCa_3$ for Thermoelectric Devices and Alternative Energy Applications. *Comput. Phys. Commun.* **2014**, *185*, 1394−1398.

(4) Madsen, G. K. H. Automated Search for New Thermoelectric Materials: The Case of LiZnSb. *J. Am. Chem. Soc.* **2006**, *128*, 12140−12146.

(5) Yang, L.; Chen, Z. G.; Dargusch, M. S.; Zou, J. High Performance Thermoelectric Materials: Progress and Their Applications. *Adv. Energy Mater.* **2018**, *8*, 1701797.

(6) Kagdada, H. L.; Jha, P. K.; Śpiewak, P.; Kurzydłowski, K. J. Structural Stability, Dynamical Stability, Thermoelectric Properties, and Elastic Properties of GeTe at High Pressure. *Phys. Rev. B* **2018**, *97*, 134105.

(7) Hong, M.; Lyv, W.; Li, M.; Xu, S.; Sun, Q.; Zou, J.; Chen, Z.-G. Rashba Effect Maximizes Thermoelectric Performance of GeTe Derivatives. *Joule* **2020**, *4*, 2030−2043.

(8) Jaziri, N.; Boughamoura, A.; Müller, J.; Mezghani, B.; Tounsi, F.; Ismail, M. A Comprehensive Review of Thermoelectric Generators: Technologies and Common Applications. *Energy Rep.* **2020**, *6*, 264−287.

(9) Dargusch, M.; Liu, W. D.; Chen, Z. G. Thermoelectric Generators: Alternative Power Supply for Wearable Electrocardiographic Systems. *Adv. Sci.* **2020**, *7*, 2001362.
(10) Zheng, Y.; Tan, X. Y.; Wan, X.; Cheng, X.; Liu, Z.; Yan, Q. Thermal Stability and Mechanical Response of Bi_2Te_3-Based Materials for Thermoelectric Applications. *ACS Appl. Energy Mater.* **2019**, *3*, 2078−2089.
(11) Guttmann, G. M.; Gelbstein, Y. Mechanical Properties of Thermoelectric Materials for Practical Applications. In *Bringing Thermoelectricity into Reality*; Aranguren, P., Ed.; IntechOpen: Rijeka, Croatia, 2018; pp 63−80.
(12) He, R.; Gahlawat, S.; Guo, C.; Chen, S.; Dahal, T.; Zhang, H.; Liu, W.; Zhang, Q.; Chere, E.; White, K.; et al. Studies on Mechanical Properties of Thermoelectric Materials by Nanoindentation. *Phys. Status Solidi A* **2015**, *212*, 2191−2195.
(13) Maynard, J. Resonant Ultrasound Spectroscopy. *Phys. Today* **1996**, *49*, 26−31.
(14) Fan, X.; Li, M. M.; Singh, D. J.; Jiang, Q.; Zheng, W. T. Identification of a Potential Superhard Compound ReCN. *J. Alloys Compd.* **2015**, *631*, 321−327.
(15) Guerrero-Sánchez, J.; Takeuchi, N.; Reyes-Serrato, A. Ab-initio Study of ReCN in the Bulk and As a New Two Dimensional Material. *Sci. Rep.* **2017**, *7*, 2799.
(16) Kokalj, A. XCrySDen-a New Program for Displaying Crystalline Structures and Electron Densities. *J. Mol. Graphics Modell.* **1999**, *17*, 176−179. . Code available from http://www.xcrysden.org/
(17) McMillan, P. F. New materials From High-Pressure Experiments. *Nat. Mater.* **2002**, *1*, 19−25.
(18) Bykov, M.; Fedotenko, T.; Chariton, S.; Laniel, D.; Glazyrin, K.; Hanfland, M.; Smith, J. S.; Prakapenka, V. B.; Mahmood, M. F.; Goncharov, A. F.; et al. High-Pressure Synthesis of Dirac Materials: Layered van der Waals Bonded BeN_4 Polymorph. *Phys. Rev. Lett.* **2021**, *126*, 175501.
(19) Markov, M.; Rezaei, S. E.; Sadeghi, S. N.; Esfarjani, K.; Zebarjadi, M. Thermoelectric Properties of Semimetals. *Phys. Rev. Mater.* **2019**, *3*, 095401.
(20) Parker, D.; Singh, D. J. High-Temperature Thermoelectric Performance of Heavily Doped PbSe. *Phys. Rev. B: Condens. Matter Mater. Phys.* **2010**, *82*, 035204.
(21) Wang, H.; Pei, Y.; LaLonde, A. D.; Snyder, G. J. Heavily Doped p-Type PbSe with High Thermoelectric Performance: An Alternative for PbTe. *Adv. Mater.* **2011**, *23*, 1366−1370.
(22) Tritt, T. M.; Subramanian, M. A. Thermoelectric Materials, Phenomena, and Applications: A Bird's Eye View. *MRS Bull.* **2006**, *31*, 188−198.
(23) Twaha, S.; Zhu, J.; Yan, Y.; Li, B. A Comprehensive Review of Thermoelectric Technology: Materials, Applications, Modelling and Performance Improvement. *Renewable Sustainable Energy Rev.* **2016**, *65*, 698−726.
(24) Zhu, X.-L.; Hou, C.-H.; Zhang, P.; Liu, P.-F.; Xie, G.; Wang, B.-T. High Thermoelectric Performance of New Two-Dimensional IV-VI Compounds: A First-Principles Study. *J. Phys. Chem. C* **2020**, *124*, 1812−1819.
(25) Zhou, W.-X.; Wu, D.; Xie, G.; Chen, K.-Q.; Zhang, G. α-Ag_2S: A Ductile Thermoelectric Material with High ZzT. *ACS Omega* **2020**, *5*, 5796−5804.
(26) Joshi, T. K.; Shukla, A.; Sharma, G.; Verma, A. S. Computational Determination of Structural, Electronic, Optical, Thermoelectric and Thermodynamic Properties of Hybrid Perovskite $CH_3CH_2NH_3GeI_3$: An Emerging Material for Photovoltaic Cell. *Mater. Chem. Phys.* **2020**, *251*, 123103.
(27) Blaha, P.; Schwarz, K.; Tran, F.; Laskowski, R.; Madsen, G. K. H.; Marks, L. D. WIEN2k: An APW+lo Program for Calculating the Properties of Solids. *J. Chem. Phys.* **2020**, *152*, 074101.
(28) Perdew, J. P.; Burke, K.; Ernzerhof, M. Generalized Gradient Approximation Made Simple. *Phys. Rev. Lett.* **1996**, *77*, 3865−3868.
(29) Togo, A.; Tanaka, I. First Principles Phonon Calculations in Materials Science. *Scr. Mater.* **2015**, *108*, 1−5.
(30) Kresse, G.; Furthmüller, J. Efficiency of Ab-Initio Total Energy Calculations for Metals and Semiconductors Using a Plane-Wave Basis Set. *Comput. Mater. Sci.* **1996**, *6*, 15−50.
(31) Kresse, G.; Furthmüller, J. Efficient Iterative Schemes for Ab Initio Total-Energy Calculations Using a Plane-Wave Basis Set. *Phys. Rev. B: Condens. Matter Mater. Phys.* **1996**, *54*, 11169−11186.
(32) Monkhorst, H. J.; Pack, J. D. Special Points for Brillouin-Zone Integrations. *Phys. Rev. B: Solid State* **1976**, *13*, 5188−5192.
(33) Madsen, G. K. H.; Singh, D. J. BoltzTraP. A Code for Calculating Band-Structure Dependent Quantities. *Comput. Phys. Commun.* **2006**, *175*, 67−71.

https://doi.org/10.1021/acsomega.1c02357
ACS Omega 2021, 6, 18364−18369